Chem. Pap.
DOI 10.1007/s11696-017-0187-7

ORIGINAL PAPER

Influence of the methylene group between azadithiolate nitrogen atom and phenyl moiety on the protophilic properties of [FeFe]-hydrogenase model complexes

Shang Gao[1] · Ting-Ting Yang[1] · Jian-Xun Zhao[1] · Qian Duan[1] · Qing-Cheng Liang[1] · Da-Yong Jiang[1]

Received: 28 December 2016 / Accepted: 2 May 2017

Abstract An [FeFe]-hydrogenase mimic **4** with functional benzyl moiety covalently linked to the azadithiolate ligand was synthesized. The structure, protonation, and electrochemical properties of **4** and a phenyl substituted analogue (coded as **3**) were simultaneously studied to explore the influence of the methylene group between the bridgehead nitrogen atom and functional phenyl moiety on the protophilic properties of the model complexes. X-ray single crystal diffraction analysis revealed that the nitrogen atoms of **3** and **4** possessed sp^2 and sp^3-hybridization, respectively. Although the light-driven electron transfer was prevented in the molecule of **4**, the sp^3-hybridized nitrogen atom of **4** could be protonated in the presence of the proton acid to give the $[\mathbf{4}(NH)]^+$ cation. The generated positive charge could be reduced at ca. −1.2 V versus Fc/Fc^+ with a distinctly electrocatalytic proton reduction activity, whereas the proton reduction catalysed by **3** occurred at ca. −1.45 V. The catalytic proton reductions of **3** and **4** followed ECCE and CECE mechanisms, respectively. It was noteworthy that the potential of **4** was remarkably anodic shifted and closer to that of the proton reduction catalysed by natural enzymes.

Keywords Hydrogenase · Enzyme mimic · Azadithiolate · Electrochemistry · Proton reduction

Introduction

Hydrogenases are a series of metalloenzymes that catalyse the reversible interconversion of protons and molecular hydrogen (Lubitz et al. 2014). According to the metal ion composition of their active sites, hydrogenases can be classified as [Fe]-, [NiFe]-, or [FeFe]-hydrogenase. All of these enzymes are of high interest in biotechnology while [FeFe]-hydrogenases are particularly active in both hydrogen production and oxidation (Birrell et al. 2016; Sommer et al. 2017). Recently, spectroscopic and crystallographic studies have revealed the organometallic nature of [FeFe]-hydrogenase active site (so-called H-cluster, Scheme 1), which consists of a butterfly [2Fe] subunit and a [4Fe4S] cluster connected via a thiolate of a cysteine residue (Peters et al. 1998; Nicolet et al. 1999). Both the [2Fe] and the [4Fe4S] sub-clusters are redox active, and the two electrons involved in the redox reaction of $2H^+ + 2e^- \leftrightarrow H_2$ are accommodated by the changing oxidation states of the two sub-clusters (Sommer et al. 2017). Possible redox states of the H-cluster such as the active oxidized state H_{ox}, the active reduced state H_{red} and the super-reduced state H_{sred} have been well characterised by combined EPR, FTIR and electrochemical studies (Lubitz et al. 2007; Adamska et al. 2012). The redox and protonation events that occurred on the [2Fe] subunit and the [4Fe4S] cluster in the catalytic cycle are also resolved in detail, demonstrating the essential necessity of the two sub-clusters (Adams 1990; Pereira et al. 2001; Adamska et al. 2012; Adamska-Venkatesh et al. 2014; Mulder et al. 2014). Inspired by the structural and functional details of H-cluster, artificial photocatalytic systems have been constructed in view of solar energy conversion (Eckenhoff and Eisenberg 2012; Wang et al. 2012; Wu et al. 2014; Wang et al. 2015). From a photochemical point of view, electron

Electronic supplementary material The online version of this article (doi:10.1007/s11696-017-0187-7) contains supplementary material, which is available to authorized users.

✉ Shang Gao
custgaoshang@126.com

[1] School of Materials Science and Engineering, Changchun University of Science and Technology, 7989 Weixing Road, Changchun 130022, People's Republic of China

Published online: 06 May 2017

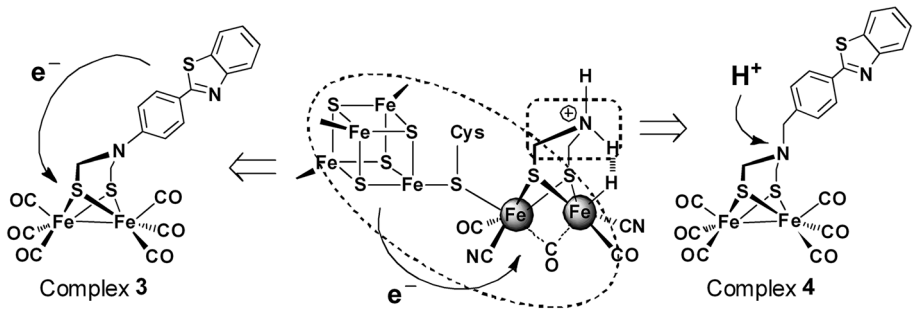

Scheme 1 Proposed intermediate in enzymatic reduction of protons and oxidation of H_2 (*middle*) and the synthetic model complexes **3** (*left*) and **4** (*right*)

transfer should be triggered by a preceding absorption of a photon by a photosensitizer. We have focused on the construction of inexpensive [FeFe]-hydrogenase mimics with photocatalytic activity (Gao et al. 2014, 2017). One successful model was complex **3** (as depicted in Scheme 1), consisting of a noble-metal-free organic chromophore, a [2Fe2S] proton reduction catalytic centre to accomplish the photo-induced H_2 evolution. The light-driven intramolecular electron transfer has been evidentially demonstrated, and a remarkably photocatalytic efficiency was achieved. However, the other significant source of reducing equivalents for converting protons to molecular hydrogen, that is, electrochemistry, has not been thoughtfully investigated.

On the other hand, the dithiol ligand has been unequivocally confirmed as an azadithiolate (Silakov et al. 2009; Erdem et al. 2011; Berggren et al. 2013). The bridging amine group plays an important role for the heterocyclic cleavage or formation of hydrogen in enzymatic process. The amine moiety close to the Fe^d ("distal" to [4Fe4S] cluster) atom with open coordination site would accept or donate a proton from a transient hydride in hydrogen production (Berggren et al. 2013; Esselborn et al. 2013; Lubitz et al. 2014), acting as a proton shuttle between the protein and the H-cluster (Sommer et al. 2017). Studies on the protonation of the amino headgroup in diiron azadithiolates might contribute to the understanding of the mechanism of enzymatic hydrogen production and/or uptake. Likewise, after protonation, the nitrogen-bridged diiron complex exhibited milder reduction potential (Ott et al. 2004; Wang et al. 2007; Jiang et al. 2007; Capon et al. 2008), which was closer to that (ca. −1.0 V versus Fc/Fc^+) of the proton reduction catalysed by natural enzymes (Holm et al. 1996; Butt et al. 1997).

Relative to the phenyl species as a substituent on the azadithiolate nitrogen atom, the benzyl group seemed to have an influence on the architectural, protonated and electrochemical properties of the diiron dithiolate complex. We, therefore, set out to synthesize a new [FeFe]-hydrogenase active site mimic which contains a functional benzyl group covalently embedded to the azadithiolate ligand (coded as **4**, Scheme 1). The structure, acid titration and cyclic voltammetry are explored to give more insights into the influence of the methylene group between the azadithiolate nitrogen atom and functional phenyl moiety on the protophilic properties of [FeFe]-hydrogenase model complex. Herein, the synthesis, structures, *N*-protonation and electrochemical properties of **4** and the phenyl substituted analogue **3** were discussed in detail.

Experiment

Reagents and instruments

All organometallic reactions and operations were carried out under a dry, oxygen-free argon atmosphere with standard Schlenk techniques. All solvents were dried and distilled prior to use by standard methods. Starting compound $[(\mu\text{-S})_2\{Fe(CO)_3\}_2]$ was prepared according to literature procedure (Bogan et al. 1983). Other materials were commercially available and used without further purification.

IR spectra were recorded on JASCO FT/IR 430 spectrophotometer. ^1H and ^{13}C spectra were collected on a Bruker AVANCE II/400 NMR spectrometer. HR-MS determinations were made on a GCT-MS instrument (Micromass, England). UV–Vis spectra were measured on a PerkinElmer Lambda 35 spectrophotometer. Steady-state emission spectra were determined on JASCO FP-6500 spectrophotometer.

Synthesis and characterization

2-[4-(bromomethyl)phenyl]benzothiazole (coded as **1a**, Scheme 2) was synthesized from 4-methylbenzoic acid and 2-aminothiophenol according to literature procedures (Palmer et al. 1971; Yoshino et al. 1986). The solution of **1a** (4.5 g, 15 mmol) in anhydrous $CHCl_3$ (50 mL) was added dropwise to a solution (40 mL anhydrous $CHCl_3$) of hexamethylenetetramine (2.1 g, 15 mmol). The mixture was refluxed for 5 h with vigorous stirring. The resulting precipitate was washed several times with deionized water and added to a mixture of ethanol and concentrated HCl

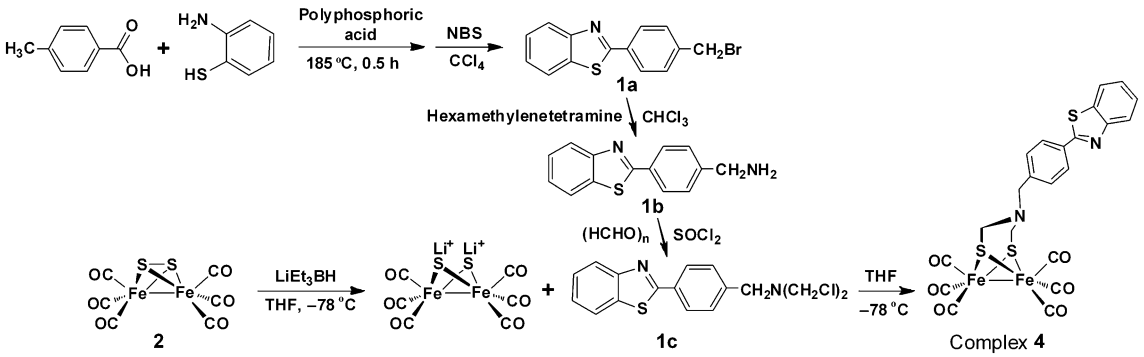

Scheme 2 Synthetic procedure of the model complex **4**

(4:1, 100 mL). The resulting solution was kept stirring at 70 °C for 12 h and then allowed to stand at room temperature overnight. An HCl salt was obtained by filtration, washed with 10% $KHCO_3$ (50 mL) and extracted into $CHCl_3$ (50 mL). The organic layer was dried over anhydrous $MgSO_4$. The solvent was removed in vacuo to give the primary amine **1b** as a yellow solid (3.06 g, 85%). A mixture of **1b** (1.8 g, 7.5 mmol) and paraformaldehyde (0.6 g, 19.5 mmol) in 20 mL CH_2Cl_2 was stirred for 5 h and treated dropwise with 2.25 mL (31 mmol) of $SOCl_2$. After 1.5 h, the solvent and unreacted $SOCl_2$ were removed under vacuum to give the product **1c**. The generated solid was added to the THF solution of $[(\mu\text{-LiS})_2Fe_2(CO)_6]$, freshly prepared by the reaction of super hydride $LiEt_3BH$ (1 mol L^{-1} solution in THF, 8 mL) and $[(\mu\text{-S})_2\text{-}\{Fe(CO)_3\}_2]$ (**2**) (1.38 g, 4 mmol in 30 mL THF). The mixture was stirred for 2 h at −78 °C and then 1 h at room temperature. The solvent was removed on a rotary evaporator. The crude product was purified by column chromatography (silica, 10% dichloromethane in hexane as eluent) to give complex **4** (1.77 g, 72%) as a red solid.

^{1}H NMR (400 MHz, $CDCl_3$): $\delta = 7.93$ (d, 2H, C_6H_4), 7.52 (s, 2H, NC_6H_4S), 7.42 (s, 2H, NC_6H_4S), 7.34 (s, 2H, C_6H_4), 3.78 (s, 2H, $PhCH_2$), 3.37 (s, 4H, SCH_2) ppm; ^{13}C NMR (100 MHz, $CDCl_3$): $\delta = 207.9$, 167.6, 154.3, 139.2, 135.2, 133.4, 129.4, 128.0, 126.6, 125.5, 123.5, 121.8, 61.7, 52.6 ppm; IR (CH_2Cl_2): $\tilde{\nu}$/cm^{-1} 2073, 2030, 1995 (CO); HR-MS (EI): m/z calc. for [M^+]: 609.8713; found: 609.8708.

Crystal structure determination

The X-ray diffractions of all single crystals were made on a SMART APEX II diffractometer. Data were collected at 273 K using graphite monochromatic Mo-K_α radiation ($\lambda = 0.71073$ Å) in the ω-2θ scan mode. Data processing was accomplished with the SAINT processing program (Siemens Energy and Automation Inc., 1996). Intensity data were corrected for absorption by the SADABS program (Sheldrick 1996). The structures were solved by direct methods and refined by full-matrix least-squares techniques on F_O^2 using the SHELXTL 97 crystallographic software package (Sheldrick 1997). All non-hydrogen atoms were refined anisotropically. All hydrogen atoms were located using the geometric method, and their positions and thermal parameters were fixed during the structure refinement. Details of crystal data, data collections and structure refinements were summarized in Table 1.

Electrochemistry

Electrochemical measurements were made with a BAS 100B electrochemical workstation at a scan rate of 100 mV s^{-1}. All voltammograms were obtained in a conventional three-electrode cell under argon and at ambient temperature. The working electrode was a glassy carbon disc (diameter 3 mm) that was successively polished with 3- and 1 μm diamond pastes and sonicated for 15 min prior to use. The reference electrode was a non-aqueous Ag/Ag^+ electrode (0.01 mol L^{-1} $AgNO_3$ and 0.1 mol L^{-1} n-Bu_4NPF_6 in CH_3CN) and the counter electrode was a platinum wire. The potentials were reported versus ferrocene (Fc)/ferrocenium (Fc^+) couple.

Results and discussion

In the present report, commercially available materials were employed to generate the target product. Bromination of 2-*p*-tolylbenzothiazole with *N*-Bromosuccinimide (NBS) gave the bromomethyl compound **1a** for subsequent reactions. Then the aminomethyl compound **1b** was prepared via a short and high-yielding procedure (Gunnlaugsson et al. 2004) instead of the classical Gabriel amine synthesis (Fyles and Suresh 1994). The transformation of **1a** with the inexpensive hexamethylenetetramine in dry chloroform was easy to yield an insoluble amine compound, which could be dissolved in a mixture of ethanol

Table 1 Crystallographic data and processing parameters for complexes **3** and **4**

Complex	**3**	**4**
Formula	$C_{21}H_{12}Fe_2N_2O_6S_3$	$C_{22}H_{14}Fe_2N_2O_6S_3$
M_w	596.21	610.23
Crystal system	Monoclinic	Orthorhombic
Space group	*P*2(1)/*c*	*P*2(1)2(1)2(1)
a (Å)	13.8606(12)	6.651(3)
b (Å)	7.6900(7)	14.208(7)
c (Å)	21.5052(19)	25.854(12)
V (Å^3)	2290.1(4)	2443.2(19)
Z	4	4
$D_{calcd.}$/g cm^{-3}	1.729	1.659
μ (mm^{-1})	1.582	1.485
F(000)	1200	1232
Crystal size (mm)	0.45 × 0.22 × 0.10	0.95 × 0.08 × 0.07
Reflns collected	12,350	11,654
Independent reflections	4509	3991
R_{int}	0.0204	0.0301
Parameters refined	307	316
GOF on F^2	1.035	0.982
R_1 [$I > 2\sigma(I)$]	0.0231	0.0270
wR_2 [$I > 2\sigma(I)$]	0.0620	0.0495
Residual electron density (e Å^{-3})	0.281/−0.232	0.223/−0.162

and concentrated HCl. After the filtration of the HCl salt, compound **1b** was isolated as a product in ca. 85% yield. The resulting primary amine could react readily with paraformaldehyde and $SOCl_2$ to generate bis(chloromethyl)amine **1c** (Lawrence et al. 2001a, b). The treatment of **1c** with $[(\mu\text{-S})_2\{Fe(CO)_3\}_2]^{2-}$ dianion, freshly derived from $[(\mu\text{-S})_2\{Fe(CO)_3\}_2]$ in THF, gave the iron thiolate carbonyl dimer **4** in a reasonable yield (Scheme 2).

Complex **4** was fully characterized by ^{1}H NMR, ^{13}C NMR, IR and HR-MS spectroscopies. The molecular structure was further confirmed by X-ray crystallography. ORTEP plots of **4** and complex **3** were shown in Fig. 1, while the selected bond lengths and angles were summarized in Table 2. Both complexes consisted of a butterfly architectonic [2Fe] core with distorted square-pyramidal geometry around each iron atom (Tard and Pickett 2009; Simmons et al. 2014). The Fe–Fe bond lengths [**3**: 2.5036(4) Å, **4**: 2.5013(12) Å] were in good agreement with those of previously reported diiron azadithiolates (2.48–2.52 Å) (Georgakaki et al. 2003; Liu et al. 2005; Tard et al. 2005; Gloaguen and Rauchfuss 2009), whereas slightly shorter than those in the structures of enzymes *Clostridium pasterianum* and *Desulfovibrio desulfuricans* (ca. 2.6 Å) (Peters et al. 1998; Nicolet et al. 1999, 2001). Indeed, the models **3** and **4** involved two fused six-membered rings in which the *N*-substituted azadithiolate ligands were η^2:η^2-coordinated to the $Fe(CO)_3$ moieties. One ring (Fe1–S1–C7–N1–C8–S2) adopted a chair conformation, while the other ring (Fe2–S1–C7–N1–C8–S2) had a boat conformation. Although the structures of the $Fe_2S_2(CO)_6$ subunits of **3** and **4** appeared quite similar, the tertiary amine moieties featured apparently distinct conformations. The substituted phenyl group of **3** lay in the axial position relative to above-mentioned metalloheterocycle, while the benzyl moiety resided in an equatorial position in **4**. In the light of the C–N–C angles, the sum of ca. 357° for **3** and 332° for **4** suggested that the bridgehead azadithiolate nitrogen atoms were sp^2 and sp^3-hybridized, respectively. It was noteworthy that N1 atom in **3** possessed a pseudo-triangular conformation, leading to slightly weakened p-π conjugation between the p-orbital of

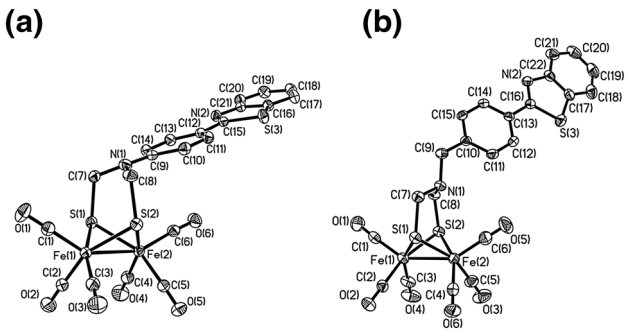

Fig. 1 Molecular structures of complexes **3** (**a**) and **4** (**b**) with 30% probability level ellipsoids (the hydrogen atoms have been omitted for clarity)

Table 2 Selected bond lengths (Å) and angles (deg) for complexes **3** and **4**

Complex	**3**	**4**
Bond lengths		
Fe(1)–Fe(2)	2.5036(4)	2.5013(12)
Fe(1)–S(1)	2.2663(5)	2.2485(11)
Fe(1)–S(2)	2.2647(5)	2.2487(11)
Fe(2)–S(1)	2.2717(5)	2.2466(11)
Fe(2)–S(2)	2.2594(5)	2.2534(11)
N(1)–C(7)	1.423(2)	1.448(4)
N(1)–C(8)	1.432(2)	1.445(3)
N(1)–C(9)	1.404(2)	1.472(3)
N(1)···C(6)	3.4891(23)	3.1781(41)
S(1)···S(2)	3.0609(6)	3.0226(17)
Bond angles		
Fe(1)–S(1)–Fe(2)	66.969(15)	67.62(3)
Fe(1)–S(2)–Fe(2)	67.201(15)	67.50(4)
S(1)–Fe(1)–Fe(2)	56.619(14)	56.15(3)
S(1)–Fe(2)–Fe(1)	56.412(13)	56.23(3)
S(2)–Fe(1)–Fe(2)	56.300(13)	56.34(3)
S(2)–Fe(2)–Fe(1)	56.499(14)	56.16(3)
C(1)–Fe(1)–Fe(2)	147.69(6)	147.16(11)
C(6)–Fe(2)–Fe(1)	154.19(6)	148.57(11)
C(7)–N(1)–C(8)	113.03(15)	111.8(2)
C(7)–N(1)–C(9)	121.62(15)	109.4(2)
C(8)–N(1)–C(9)	122.20(15)	110.7(2)
Dihedral[a]	71.7	78.5

[a] Defined by the intersection of the two SFe_2 planes

nitrogen atom and the phenyl ring. On the other hand, the sp^3-hybridized N1 atom in **4** holds a distorted tetrahedral conformation with the nitrogen lone-pair pointing towards Fe2 nucleus. The nonbonding C···N distance between the azadithiolate nitrogen atom and the nearest carbonyl carbon atom was significantly shortened in **4** (ca. 3.18 Å) than in **3** (ca. 3.49 Å).

Protonation of **4** occurred in the CH_3CN solution upon addition of a strong organic acid such as triflic acid (HOTf, $pK_a \sim 2.6$ in CH_3CN) (Eilers et al. 2007). Complex **4** in CH_3CN solution exhibited three characteristic $\tilde{\nu}$(CO) bands at 2073, 2030 and 1995 cm^{-1} in IR spectrum (Fig. 2a). Addition of an excess of HOTf to the CH_3CN solution of **4** resulted in a shift of $\tilde{\nu}$(CO) bands to higher frequencies with an average value of ca. 18 cm^{-1} (Fig. 2b), which represented a protonation of the azadithiolate nitrogen (Lawrence et al. 2001a, b; Schwartz et al. 2006) and a generation of *N*-protonated product **4**(NH). Subsequent titration of an organic base such as triethanolamine (TEOA) revealed that the protonation and deprotonation

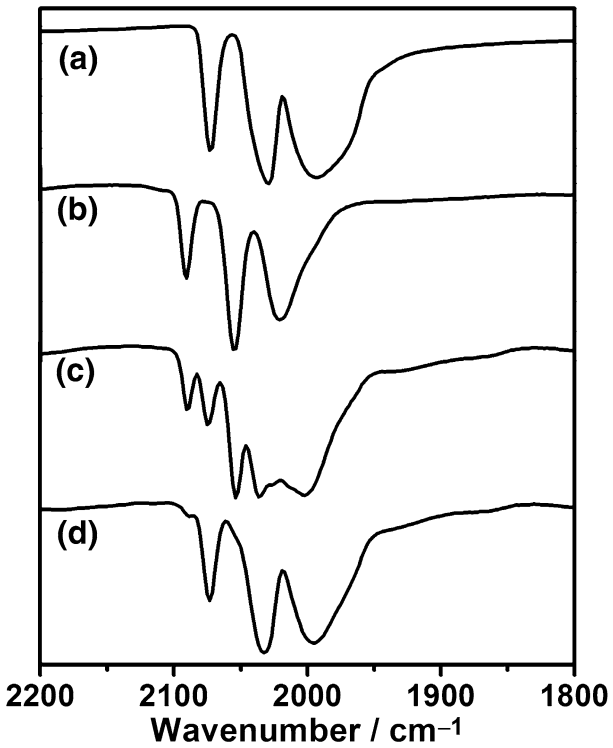

Fig. 2 FT-IR spectra of (**a**) **4** in CH_3CN, (**b**) **4** + 5 equiv. of HOTf in CH_3CN, (**c**) **4**(NH) + 0.5 equiv. of TEOA in CH_3CN, (**d**) **4**(NH) + 1 equiv. of TEOA in CH_3CN

processes of **4** and **4**(NH) were reversible. With the addition of 0.5 equiv. of TEOA to the CH_3CN solution of **4**(NH), the $\tilde{\nu}$(CO) bands of **4** recovered while the $\tilde{\nu}$(CO) bands of **4**(NH) still existed (Fig. 2c), indicative of the equilibrium between **4** and **4**(NH). Further addition of TEOA up to 1 equiv. resulted in quantitative recovery of **4**. The $\tilde{\nu}$(CO) absorptions shifted to the frequencies essentially equal to those of **4** (Fig. 2d). Meanwhile, addition of strong acid to solutions of the related phenyl-substituted analogue **3** did not result in the changed IR spectra, suggesting that the bridgehead nitrogen atom of **3** could not be protonated under present conditions.

The UV/Vis spectrum of complex **4** was dominated by an intense absorption band in the UV region around 315 nm, which could be attributed to the π–π* excitation within the phenylbenzothiazole chromophore (Fig. 3a). A low-energy shoulder was visible in the near UV region and featured σ–σ* and d–σ* character involved with the [2Fe] unit (Goy et al. 2013). The metal-based band determined the photophysical and photochemical properties of **4**. Likewise, a broad and featureless absorption reaching up to 550 nm was similar to the characteristic bands of previously reported [FeFe]-hydrogenase mimics (Eilers et al. 2007) and was responsible for the dark red colour of **4** solution. Excitation of the π–π* absorption of **4** resulted in a fluorescence emission band around 370 nm, with a much

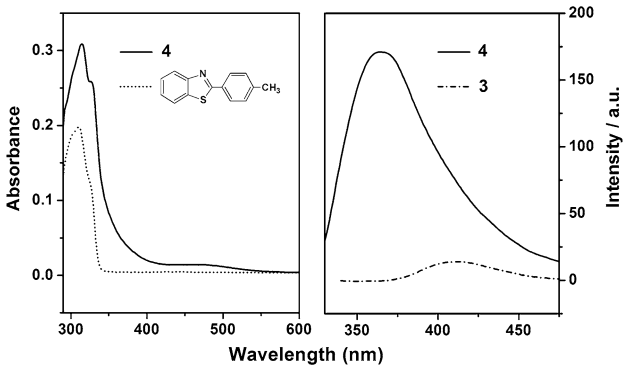

Fig. 3 UV-Vis absorption (*left*) and emission (*right*) spectra of complexes **3**, **4**, and compound 2-*p*-tolylbenzothiazole, recorded in CH_3CN

stronger emission intensity relative to that of **3** (Fig. 3b). We had demonstrated that the luminescence quenching of complex **3** was caused by the intramolecular oxidative process with electron transfer from the excited chromophore to [2Fe] unit in **3** (Gao et al. 2014). Such an intramolecular electron transfer was recognized as one of the important steps required for light-driven reduction of protons to hydrogen performed by [FeFe]-hydrogenase mimic. The differences in emissions between **3** and **4** suggested that the desirable electron transfer might be prevented in latter molecule. It could be concluded that the short rigid architecture of **3** was more favourable for the light-driven intramolecular electron transfer.

The electrochemical behaviours of **3** and **4** were investigated by cyclic voltammetry (CV) in CH_3CN with *n*-Bu_4NPF_6 (0.05 mol L^{-1}) as supporting electrolyte under an argon atmosphere (Fig. 4). All potentials were in volts versus Fc/Fc^+. In dry solution, **3** and **4** exhibited similar reduction processes, with one quasi-reversible (−1.53 V for **3**, −1.60 V for **4**) and an irreversible reduction peak (−1.96 V for **3**, −2.03 V for **4**). The primary reduction

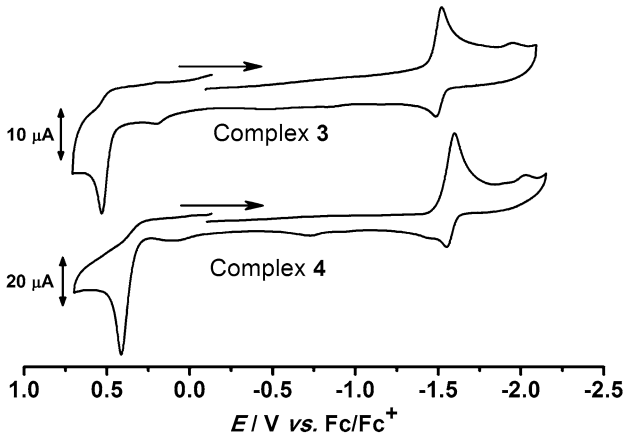

Fig. 4 CVs of complexes **3** and **4** in CH_3CN solution (0.05 mol L^{-1} *n*-Bu_4NPF_6). The scan rate is 100 mV s^{-1}

event might involve the transfer of two electrons occurred at closely separated potentials (Borg et al. 2004; Capon et al. 2007, 2009; Felton et al. 2007, 2009a) or the two-electron processes coupled with chemical reaction (Zeng et al. 2010; Xiao et al. 2011; Zhao et al. 2012; Qian et al. 2015). In either case, the redox process of $[Fe^IFe^I]$ to $[Fe^IFe^0]$ undoubtedly occurred around −1.53 V for **3** and −1.60 V for **4**. Likewise, electrochemically irreversible oxidation events had been established at 0.53 V for **3** and 0.41 V for **4**. The ratios of the oxidation peak current of **3** and **4** over the primary reduction peak current were both ca. 1.5. Hereby, we assumed the oxidations of **3** and **4** to be combined results of two overlapping processes of $[Fe^IFe^I]$ to $[Fe^IFe^{II}]$ and the oxidation of phenylbenzothiazole moiety. Moreover, the redox potential could be usually considered as an indicator to detect the electron density around the iron nuclei in [FeFe]-hydrogenase mimics. The more negative reduction potentials and less positive oxidation potential of **4** relative to those of **3** indicated that **4** was easier to be oxidized and carried a decreased reduction capability. The azadithiolate nitrogen atom of **3** was part of an aniline. The N lone pair could overlap with the two antibonding σ^*_{C-S} orbitals to form an orbital mixing that represented the hyperconjugation. The hyperconjugation effect led to a relatively strong communication between the azadithiolate nitrogen atom and the [2Fe] site, which was responsible for the more positive reduction potential of **3**.

The electrocatalytic proton reduction of complexes **3** and **4** were studied by CV in the presence of *p*-toluenesulfonic acid (HOTs, pK_a ~8.0 in CH_3CN) (Fujinaga and Sakamoto 1977) with the concentration of 2–8 mM. Upon addition of 2 equiv. of HOTs to the CH_3CN solution of **3**, a new reduction event was observed at ca. −1.45 V while the peak of the initial $[Fe^IFe^I]/[Fe^IFe^0]$ reduction process at ca. −1.53 V still existed. The current intensity of the former reduction exhibited a well linear increase with sequential increments of the acid concentration, while the potential slightly shifted towards a more negative value (Fig. 5). These electrochemical behaviours featured a catalytic proton reduction process (Bhugun et al. 1996; Gloaguen et al. 2001) and demonstrated the electrocatalytic activity of **3**. Moreover, the CVs did not display any largely anodic shifted peak in the whole process, implying that the protonation of azadithiolate nitrogen atom of **3** had not taken place in the catalytic proton reduction (vide infra).

Based on aforementioned electrochemical observations and other similar cases (Capon et al. 2005, 2009; Felton et al. 2009b), an ECCE (electrochemical–chemical–chemical–electrochemical) process could be proposed to account for the proton reduction catalysed by **3** in the presence of HOTs. Initially, the azadithiolate $[Fe^IFe^I]$ complex **3** was reduced at ca. −1.53 V to give the $[Fe^0Fe^I]^-$ monoanion (1st E step). In the presence of proton acid, the $[Fe^0Fe^I]^-$

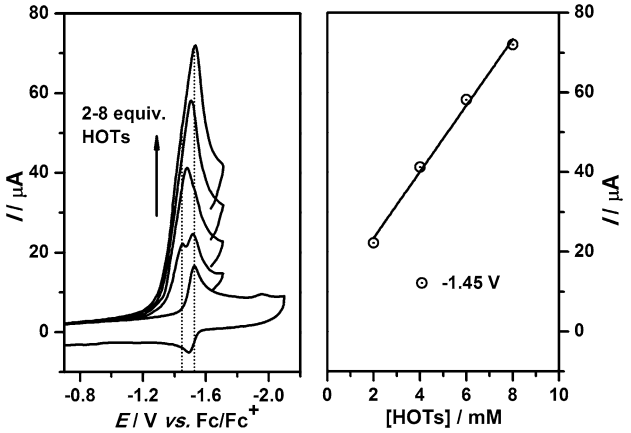

Fig. 5 *Left* CVs of complex **3** in $CH_3CN/n\text{-}Bu_4NPF_6$ solution in the absence and presence of 2, 4, 6, 8 equiv. of HOTs. The scan rate is 100 mV s^{-1}. *Right* Dependence of current intensity of the electrocatalytic reductions on the concentration of HOTs

species accepted a proton (1st C step) and underwent a subsequent protonation to form the η^2-H_2 species (2nd C step), which could be reduced at the potential (−1.45 V) slightly more positive than −1.53 V (2nd E step) to release molecular hydrogen and accomplish the electrocatalytic proton reduction cycle.

In contrast to the electrochemical behaviours of complex **3**, addition of HOTs to the solution of **4** in CH_3CN resulted in new reduction peak at ca. −1.2 V being observed (Fig. 6). The peak was shifted by around 0.4 V towards more positive potential relative to the primary reduction of **4** and could be ascribed to a one-electron reduction process of the introduced $[\mathbf{4}(NH)]^+$ cation. The difference between the reduction potentials of $[\mathbf{4}(NH)]^+$ and **4** was consistent with those found for previously reported azadithiolate diiron analogues (Ott et al. 2004; Wang et al. 2007; Jiang et al. 2007; Capon et al. 2008) and implied that the protonation occurred at the azadithiolate nitrogen atom rather than at the Fe–Fe bond, which generally resulted in larger potential shifts (Zhao et al. 2002; Gloaguen et al. 2002; Eilers et al. 2007). The current of the peak at −1.2 V increased linearly with the amount of acid added (2–8 equiv.), indicative of the catalytic reduction of protons at this potential. Likewise, an acid-dependent reduction around −1.54 V had also been evidenced. The slopes of the plots of current versus acid concentration showed that the process observed around −1.54 V exhibited a slightly greater catalytic activity.

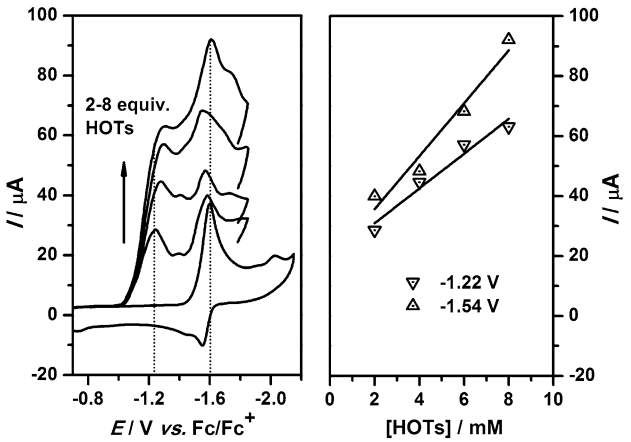

Fig. 6 *Left* CVs of complex **4** in $CH_3CN/n\text{-}Bu_4NPF_6$ solution in the absence and presence of 2, 4, 6, 8 equiv. of HOTs. The scan rate is 100 mV s^{-1}. *Right* Dependence of current intensity of the electrocatalytic reductions on the concentration of HOTs

Obviously, the catalytic proton reduction of **4** followed a distinguishing mechanism relative to that of **3**. The presence of the moderately strong acid (HOTs) resulted in the protonation of azadithiolate nitrogen atom of **4** (1st C step). The generated $[\mathbf{4}(NH)]^+$ was electrochemically reduced to **4**(NH) at ca. −1.2 V (1st E step). The metal-centred reduction likely increased the electron density of the diiron site significantly so that HOTs was able to protonate **4**(NH) at the electron-rich Fe–Fe bond, producing a cationic complex with a bridging hydride ligand (2nd C step). The μ-hydride diiron complex underwent a second reduction at a potential close to that of $[\mathbf{4}(NH)]^+$ (2nd E step), and then the catalyst was liberated and made available for another cycle. The catalytic cycle was proposed to be a CECE process for the reduction behaviours of **4** at ca. −1.2 V. However, the mechanism of the proton reduction path observed around −1.54 V was somewhat complicated, and the related investigations are now underway.

Conclusions

In summary, a functional benzyl-containing diiron azadithiolate complex (coded as **4**) was synthesized as biomimetic model of the active site of [FeFe]-hydrogenase. The structure of synthetic mimic was fully characterized by NMR, IR, HRMS spectra and X-ray single crystal diffraction analysis. Complex **4** exhibited distinct protophilic property relative to the phenyl substituted analogue (coded as **3**), due to the existence of the methylene group near the azadithiolate nitrogen atom. IR spectra evidenced that the sp^3-hybridized nitrogen atom of **4** underwent a protonation in the presence of organic acid, which did not occur for the case of **3** under same conditions. The redox behaviours of **3** and **4** in the absence of proton acid were quite similar. The most remarkable feature of **4** as a catalyst for electrochemical proton reduction was the relatively mild potential (ca. −1.2 V versus Fc/Fc^+). The potential shifted towards more positive value by ca. 250 mV related to that of **3**, which could be rationalized by considering the altered catalytic mechanism. The catalytic cycle proposed

for **4** commenced with the protonation of the azadithiolate nitrogen atom, operated at moderately negative potential and resembled the natural enzymes more closely.

Acknowledgements We are grateful to the National Natural Science Foundation of China (Nos. 21201022, 61106050), the Specialized Research Fund for the Doctoral Program of Higher Education (New Teachers, No. 20122216120001), and the Scientific and Technological Development Project of Jilin Province (No. 20150311086YY) for financial support.

References

Adams MWW (1990) The structure and mechanism of iron-hydrogenases. Biochim Biophys Acta Bioenerg 1020(2):115–145. doi:10.1016/0005-2728(90)90044-5

Adamska A, Silakov A, Lambertz C, Rüdiger O, Happe T, Reijerse E, Lubitz W (2012) Identification and characterization of the "Super-Reduced" state of the H-cluster in [FeFe] hydrogenase: a new building block for the catalytic cycle? Angew Chem Int Ed 51(46):11458–11462. doi:10.1002/anie.201204800

Adamska-Venkatesh A, Krawietz D, Siebel J, Weber K, Happe T, Reijerse E, Lubitz W (2014) New redox states observed in [FeFe] hydrogenases reveal redox coupling within the H-Cluster. J Am Chem Soc 136(32):11339–11346. doi:10.1021/ja503390c

Berggren G, Adamska A, Lambertz C, Simmons TR, Esselborn J, Atta M, Gambarelli S, Mouesca JM, Reijerse E, Lubitz W, Happe T, Artero V, Fontecave M (2013) Biomimetic assembly and activation of [FeFe]-hydrogenases. Nature 499:66–69. doi:10.1038/nature12239

Bhugun I, Lexa D, Savéant JM (1996) Homogeneous catalysis of electrochemical hydrogen evolution by iron(0) porphyrins. J Am Chem Soc 118(16):3982–3983. doi:10.1021/ja954326x

Birrell JA, Wrede K, Pawlak k, Rodriguez-Maciá P, Rüdiger O, Reijerse EJ, Lubitz W (2016) Artificial maturation of the highly active heterodimeric [FeFe] hydrogenase from *Desulfovibrio desulfuricans* ATCC 7757. Isr J Chem 56(9–10):852–863. doi:10.1002/ijch.201600035

Bogan LE, Lesch DA, Rauchfuss TB (1983) Synthesis of heterometallic cluster compounds from $Fe_3(\mu 3\text{-}Te)_2(CO)_9$ and comparisons with analogous sulfide clusters. J Organomet Chem 250(1):429–438. doi:10.1016/0022-328X(83)85067-0

Borg SJ, Behrsing T, Best SP, Razavet M, Liu XM, Pickett CJ (2004) Electron transfer at a dithiolate-bridged diiron assembly: electrocatalytic hydrogen evolution. J Am Chem Soc 126(51):16988–16999. doi:10.1021/ja045281f

Butt JN, Filipiak M, Hagen WR (1997) Direct electrochemistry of *Megasphaera elsdenii* iron hydrogenase: definition of the enzyme's catalytic operating potential and quantitation of the catalytic behaviour over a continuous potential range. Eur J Biochem 245(1):116–122. doi:10.1111/j.1432-1033.1997.00116.x

Capon JF, Gloaguen F, Schollhammer P, Talarmin J (2005) Catalysis of the electrochemical H_2 evolution by di-iron sub-site models. Coord Chem Rev 249(15–16):1664–1676. doi:10.1016/j.ccr.2004.11.018

Capon JF, Ezzaher S, Gloaguen F, Pétillon FY, Schollhammer P, Talarmin J, Davin TJ, McGrady JE, Muir KW (2007) Electrochemical and theoretical investigations of the reduction of $[Fe_2(CO)_5L\{\mu\text{-}SCH_2XCH_2S\}]$ complexes related to [FeFe] hydrogenase. New J Chem 31(12):2052–2064. doi:10.1039/B709273C

Capon JF, Ezzaher S, Gloaguen F, Pétillon FY, Schollhammer P, Talarmin J (2008) Electrochemical insights into the mechanisms of proton reduction by $[Fe_2(CO)_6\{\mu\text{-}SCH_2N(R)CH_2S\}]$ complexes related to the $[2Fe]_H$ subsite of [FeFe]hydrogenase. Chem Eur J 14(6):1954–1964. doi:10.1002/chem.200701454

Capon JF, Gloaguen F, Petillon FY, Schollhammer P, Talarmin J (2009) Electron and proton transfers at diiron dithiolate sites relevant to the catalysis of proton reduction by the [FeFe]-hydrogenases. Coord Chem Rev 253(9–10):1476–1494. doi:10.1016/j.ccr.2008.10.020

Eckenhoff WT, Eisenberg R (2012) Molecular systems for light driven hydrogen production. Dalton Trans 2012(41):13004–13021. doi:10.1039/c2dt30823a

Eilers G, Schwartz L, Stein M, Zampella G, De Gioia L, Ott S, Lomoth R (2007) Ligand versus metal protonation of an iron hydrogenase active site mimic. Chem Eur J 13(25):7075–7084. doi:10.1002/chem.200700019

Erdem ÖF, Schwartz L, Stein M, Silakov A, Kaur-Ghumaan S, Huang P, Ott S, Reijerse EJ, Lubitz W (2011) A model of the [FeFe] hydrogenase active site with a biologically relevant azadithiolate bridge: a spectroscopic and theoretical investigation. Angew Chem Int Ed 50(6):1439–1443. doi:10.1002/anie.201006244

Esselborn J, Lambertz C, Adamska-Venkatesh A, Simmons T, Berggren G, Noth J, Siebel J, Hemschemeier A, Artero V, Reijerse E, Fontecave M, Lubitz W, Happe T (2013) Spontaneous activation of [FeFe]-hydrogenases by an inorganic [2Fe] active site mimic. Nat Chem Biol 9:607–609. doi:10.1038/nchembio.1311

Felton GAN, Vannucci AK, Chen JZ, Lockett LT, Okumura N, Petro BJ, Zakai UI, Evans DH, Glass RS, Lichtenberger DL (2007) Hydrogen generation from weak acids: electrochemical and computational studies of a diiron hydrogenase mimic. J Am Chem Soc 129(41):12521–12530. doi:10.1021/ja073886g

Felton GAN, Petro BJ, Glass RS, Lichtenberger DL, Evans DH (2009a) One- to two-electron reduction of an [FeFe]-hydrogenase active site mimic: the critical role of fluxionality of the [2Fe2S] core. J Am Chem Soc 131(32):11290–11291. doi:10.1021/ja904520x

Felton GAN, Mebi CA, Petro BJ, Vannucci AK, Evans DH, Glass RS, Lichtenberger DL (2009b) Review of electrochemical studies of complexes containing the Fe_2S_2 core characteristic of [FeFe]-hydrogenases including catalysis by these complexes of the reduction of acids to form dihydrogen. J Organomet Chem 694(17):2681–2699. doi:10.1016/j.jorganchem.2009.03.017

Fujinaga T, Sakamoto I (1977) Electrochemical studies of sulfonates in non-aqueous solvents: part III. Trifluoromethanesulfonic acid as a strong acid in dipolar aprotic solvents and acetic acid. J Electroanal Chem 85(1):185–201. doi:10.1016/S0022-0728(77)80163-0

Fyles TM, Suresh VV (1994) Photoionophores derived from crown ether polycarboxylic acids: synthesis, ion binding, and spectroscopic characterization. Can J Chem 72(5):1254–1261. doi:10.1139/v94-159

Gao S, Huang S, Duan Q, Hou JH, Jiang DY, Liang QC, Zhao JX (2014) Iron–iron hydrogenase active subunit covalently linking to organic chromophore for light-driven hydrogen evolution. Int J Hydrog Energy 39(20):10434–10444. doi:10.1016/j.ijhydene.2014.05.003

Gao S, Zhang WY, Duan Q, Liang QC, Jiang DY, Zhao JX, Hou JH (2017) An artificial [FeFe]-hydrogenase mimic with organic chromophore-linked thiolate bridges for the photochemical production of hydrogen. Chem Pap 71(3):617–625. doi:10.1007/s11696-016-0049-8

Georgakaki IP, Thomson LM, Lyon EJ, Hall MB, Darensbourg MY (2003) Fundamental properties of small molecule models of Fe-only hydrogenase: computations relative to the definition of an entatic state in the active site. Coord Chem Rev 238–239:255–266. doi:10.1016/S0010-8545(02)00326-0

Gloaguen F, Rauchfuss TB (2009) Small molecule mimics of hydrogenases: hydrides and redox. Chem Soc Rev 38(1):100–108. doi:10.1039/B801796B

Gloaguen F, Lawrence JD, Rauchfuss TB (2001) Biomimetic hydrogen evolution catalyzed by an iron carbonyl thiolate. J Am Chem Soc 123(38):9476–9477. doi:10.1021/ja016516f

Gloaguen F, Lawrence JD, Rauchfuss TB, Bénard M, Rohmer MM (2002) Bimetallic carbonyl thiolates as functional models for Fe-only hydrogenases. Inorg Chem 41(4):6573–6582. doi:10.1021/ic025838x

Goy R, Apfel U, Elleouet C, Escudero D, Elstner M, Görls H, Talarmin J, Schollhammer P, González L, Weigand W (2013) A silicon-heteroaromatic system as photosensitizer for light-driven hydrogen production by hydrogenase mimics. Eur J Inorg Chem 2013(25):4466–4472. doi:10.1002/ejic.201300537

Gunnlaugsson T, Davis AP, Hussey GM, Tierney J, Glynn M (2004) Design, synthesis and photophysical studies of simple fluorescent anion PET sensors using charge neutral thiourea receptors. Org Biomol Chem 2(13):1856–1863. doi:10.1039/B404706K

Holm RH, Kennepohl PJ, Solomon EI (1996) Structural and functional sspects of metal sites in biology. Chem Rev 96(7):2239–2314. doi:10.1021/cr9500390

Jiang S, Liu J, Shi Y, Wang Z, Åkermark B, Sun LC (2007) Fe–S complexes containing five-membered heterocycles: novel models for the active site of hydrogenases with unusual low reduction potential. Dalton Trans 2007(8):896–902. doi:10.1039/B615037C

Lawrence JD, Li H, Rauchfuss TB (2001a) Beyond Fe-only hydrogenases: *N*-functionalized 2-aza-1,3-dithiolates $Fe_2[(SCH_2)_2NR](CO)_x$ ($x = 5$, 6). Chem Commun 2006(16):1482–1483. doi:10.1039/B104195A

Lawrence JD, Li H, Rauchfuss TB, Bénard M, Rohmer MM (2001b) Diiron azadithiolates as models for the iron-only hydrogenase active site: synthesis, structure, and stereoelectronics. Angew Chem Int Ed 40(9):1768–1771. doi:10.1002/1521-3773(20010504)40:9<1768:AID-ANIE17680>3.0.CO;2-E

Liu XM, Ibrahim SK, Tard C, Pickett CJ (2005) Iron-only hydrogenase: synthetic, structural and reactivity studies of model compounds. Coord Chem Rev 249(15–16):1641–1652. doi:10.1016/j.ccr.2005.04.009

Lubitz W, Reijerse E, van Gastel M (2007) [NiFe] and [FeFe] hydrogenases studied by advanced magnetic resonance techniques. Chem Rev 107(10):4331–4365. doi:10.1021/cr050186q

Lubitz W, Ogata H, Rüdiger O, Reijerse E (2014) Hydrogenases. Chem Rev 114(8):4081–4148. doi:10.1021/cr4005814

Mulder DW, Ratzloff MW, Bruschi M, Greco C, Koonce E, Peters JW, King PW (2014) Investigations on the role of proton-coupled electron transfer in hydrogen activation by [FeFe]-hydrogenase. J Am Chem Soc 136(43):15394–15402. doi:10.1021/ja508629m

Nicolet Y, Piras C, Legrand P, Hatchikian EC, Fontecilla-Camps JC (1999) *Desulfovibrio desulfuricans* iron hydrogenase: the structure shows unusual coordination to an active site Fe binuclear center. Structure 7(1):13–23. doi:10.1016/S0969-2126(99)80005-7

Nicolet Y, Lacey AL, Vernède X, Fernandez VM, Hatchikian EC, Fontecilla-Camps JC (2001) Crystallographic and FTIR spectroscopic evidence of changes in Fe coordination upon reduction of the active site of the Fe-only hydrogenase from *Desulfovibrio desulfuricans*. J Am Chem Soc 123(8):1596–1601. doi:10.1021/ja0020963

Ott S, Kritikos M, Åkermark B, Sun LC, Lomoth R (2004) A biomimetic pathway for hydrogen evolution from a model of the iron hydrogenase active site. Angew Chem Int Ed 43(8):1006–1009. doi:10.1002/anie.200353190

Palmer PJ, Hall G, Trigg RB, Warrington JV (1971) Antimicrobials. 1. Benzothiazolylbenzylamines. J Med Chem 14(12):1223–1225. doi:10.1021/jm00294a024

Pereira AS, Tavares P, Moura I, Moura JJG, Huynh BH (2001) Mössbauer characterization of the iron–sulfur clusters in *Desulfovibrio vulgaris* hydrogenase. J Am Chem Soc 123(12):2771–2782. doi:10.1021/ja003176+

Peters JW, Lanzilotta WN, Lemon BJ, Seefeldt LC (1998) X-ray crystal structure of the Fe-only hydrogenase (CpI) from *Clostridium pasteurianum* to 1.8 Angstrom resolution. Science 282(5395):1853–1858. doi:10.1126/science.282.5395.1853

Qian GF, Wang HL, Zhong W, Liu XM (2015) Electrochemical investigation into the electron transfer mechanism of a diiron hexacarbonyl complex bearing a bridging naphthalene moiety. Electrochim Acta 163:190–195. doi:10.1016/j.electacta.2015.02.163

Schwartz L, Eilers G, Eriksson L, Gogoll A, Lomoth R, Ott S (2006) Iron hydrogenase active site mimic holding a proton and a hydride. Chem Commun 2006(5):520–522. doi:10.1039/B514280F

Sheldrick GM (1996) SADABS absorption correction program. University of Göffingen, Göffingen

Sheldrick GM (1997) SHELXTL 97 program for the refinement of crystal structure. University of Göffingen, Göffingen

Siemens Energy & Automation Inc, Inc Automation (1996) Software packages SMART and SAINT. Siemens Energy & Automation Inc, Inc Automation, Madison

Silakov A, Wenk B, Reijerse E, Lubitz W (2009) ^{14}N HYSCORE investigation of the H-cluster of [FeFe] hydrogenase: evidence for a nitrogen in the dithiol bridge. Phys Chem Chem Phys 11(31):6592–6599. doi:10.1039/b905841a

Simmons TR, Berggren G, Bacchi M, Fontecave M, Artero V (2014) Mimicking hydrogenases: from biomimetics to artificial enzymes. Coord Chem Rev 270–271:127–150. doi:10.1016/j.ccr.2013.12.018

Sommer C, Adamska-Venkatesh A, Pawlak K, Birrell JA, Rüdiger O, Reijerse EJ, Lubitz W (2017) Proton coupled electronic rearrangement within the H-cluster as an essential step in the catalytic cycle of [FeFe] hydrogenases. J Am Chem Soc 139(4):1440–1443. doi:10.1021/jacs.6b12636

Tard C, Pickett CJ (2009) Structural and functional analogues of the active sites of the [Fe]-, [NiFe]-, and [FeFe]-hydrogenases. Chem Rev 109(6):2245–2274. doi:10.1021/cr800542q

Tard C, Liu XM, Ibrahim SK, Bruschi M, De Gioia L, Davies SC, Yang X, Wang LS, Sawers G, Pickett CJ (2005) Synthesis of the H-cluster framework of iron-only hydrogenase. Nature 433:610–613. doi:10.1038/nature03298

Wang F, Wang M, Liu X, Jin K, Dong W, Sun LC (2007) Protonation, electrochemical properties and molecular structures of halogen-functionalized diiron azadithiolate complexes related to the active site of iron-only hydrogenases. Dalton Trans 2007(34):3812–3819. doi:10.1039/B706178A

Wang F, Wang WG, Wang HY, Si G, Tung CH, Wu LZ (2012) Artificial photosynthetic systems based on [FeFe]-hydrogenase mimics: the road to high efficiency for light-driven hydrogen evolution. ACS Catal 2(3):407–416. doi:10.1021/cs200458b

Wang M, Han K, Zhang S, Sun LC (2015) Integration of organometallic complexes with semiconductors and other nanomaterials for photocatalytic H_2 production. Coord Chem Rev 287:1–14. doi:10.1016/j.ccr.2014.12.005

Wu LZ, Chen B, Li ZJ, Tung CH (2014) Enhancement of the efficiency of photocatalytic reduction of protons to hydrogen via molecular assembly. Acc Chem Res 47(7):2177–2185. doi:10.1021/ar500140r

Xiao ZY, Wei ZH, Long L, Wang YL, Evans DJ, Liu XM (2011) Diiron carbonyl complexes possessing a Fe(II)Fe(II) core:

synthesis, characterisation, and electrochemical investigation. Dalton Trans 40(16):4291–4299. doi:10.1039/C0DT01465F

Yoshino K, Kohno T, Uno T, Morita T, Tsukamoto G (1986) Organic phosphorus compounds. 1. 4-(Benzothiazol-2-yl)benzylphosphonate as potent calcium antagonistic vasodilator. J Med Chem 29(5):820–825. doi:10.1021/jm00155a037

Zeng XH, Li ZM, Xiao ZY, Wang YW, Liu XM (2010) Using pendant ferrocenyl group(s) as an intramolecular standard to probe the reduction of diiron hexacarbonyl model complexes for the sub-unit of [FeFe]-hydrogenase. Electrochem Commun 12(3):342–345. doi:10.1016/j.elecom.2009.12.023

Zhao X, Hsiao YM, Reibenspies JH, Darensbourg MY (2002) Oxidative addition of phosphine-tethered thiols to iron carbonyl: binuclear phosphinothiolate complexes, (μ-SCH2CH2PPh2)2Fe2(CO)4, and hydride derivatives. Inorg Chem 41(4):699–708. doi:10.1021/ic010741g

Zhao J, Wei ZH, Zeng XH, Liu XM (2012) Three diiron complexes bearing an aromatic ring as mimics of the diiron subunit of [FeFe]-hydrogenase: synthesis, electron transfer and coupled chemical reactions. Dalton Trans 41(36):11125–11133. doi:10.1039/C2DT31083J